XLI CILAMCE
XLI Ibero-Latin American Congress on Computational Methods in Engineering
16-19 November, 2020 FOZ DO IGUAÇU PARANÁ - BRAZIL

Structural Topology Optimization Applied to Scarifier Subsoiler

Artur F. de Vito Jr.[1,a], William M. Vicente[1,b]

[1]*Dept. of Agricultural Machinery, School of Agricultural Engineering, University of Campinas*
Av. Cândido Rondon, 501, 13083-875, São Paulo/Campinas, Brazil
[a]*artur.junior@feagri.unicamp.br,* [b]*william.vicente@unicamp.br*

Abstract. The subsoiler is one of the most used tools in tillage, mainly in the subsurface layers, helping in the availability of nutrients for the plants and reducing soil compaction. In some cases, this tool is oversized due to the lack of engineering tools and technical knowledge. In this aspect, this work aims to apply the topology optimization method to the shank of a subsoiler to decrease the consumption of raw material while maintaining performance during tillage. It was used Ansys, to solve the finite element analysis, in parallel with Matlab based in Bi-directional Evolutionary Structural Optimization (BESO) scheme for the compliance minimization and considering the volume as the constraint. The three-dimensional model of the subsoiler shank was generated on 3D Computer-aided design (CAD). MatLab reads the set parameters, builds an Ansys input file, and sends it to Ansys to perform the finite element analysis. Ansys exports geometry details and elemental strain energy necessary to perform the topology optimization. As a result, the topology optimized subsoiler shank is is 25% lighter than the original part with a 8% increase in the mean compliance . An adaptation of the final geometry was implemented so that the subsoiler could be more easily manufactured after applying the topological optimization method.

Keywords: BESO, Agricultural Machinery, ANSYS, Matlab

1 Introduction

Full tillage or partial tillage plays an important role in agriculture, directly in the chemical, physical and biological effects on the soil [1], it is an important stage for sustainable agriculture [2], reducing soil compaction, promoting greater availability of water and nutrients for crops. In this sense, the search for improvements and technological advances in agricultural machinery proved necessary for farmers to remain competitive [3]. Subsoiler Fig. 1 is an equipment used in tillage subject to high loads due to the soil resistance during tillage and working depth. Due to the lack of use of engineering tools and in-depth knowledge, manufacturers choose to manufacture heavy and unnecessarily strong tools [4] to avoid repeated testing with new equipment. Thus, the importance of the steps that precede the manufacture of machinery is highlighted, seeking to reduce costs and maximize the performance of equipment and structures.

Topology optimization is a computational tool used to obtain the initial optimized design of structures or equipment, obeying an objective function and boundary conditions stipulated by the user, considering the existence of pores in the continuous medium [5]. The method called Evolutionary Structural Optimization (ESO) introduced the empirical concept of removing finite elements to achieve the objective function [6], obeying the restrictions. Later, ESO evolved into a method called Bi-directional evolutionary structural optimization (BESO) [7], which in addition to removing elements, also adds them. The use of topological optimization as a computational tool has been successfully applied in biomechanical morphogenesis [8], vehicular structures [9, 10], aerospace [11], agriculture [12] and others.

Topology optimization can be helpful to bring more technological designs in agriculture. Thus, the objective of this work is to present a methodology framework capable of solving a topology optimization problem using BESO applied to a subsoiler shank.

Figure 1. John Deere subsoiler Frontier™ Shank Rippers, available in: `https://www.deere.com/en/attachments-accessories-and-implements/utility-tractors-attachments-accessories/tillage-equipment/sr12-series-shank-rippers/`

2 Methods

Mathematically the optimization problem presented in this work can be described as minimization of compliance subject to the system's equilibrium equation and also to a pre-established final volume (eq. (1)).

$$\begin{aligned} \min \quad & C = \frac{1}{2} u^T K u \\ \text{s.t.} \quad & F = Ku \\ & V_f = \frac{\sum_{i=1}^{n} V_i x_i}{\sum_{i=1}^{n} V_i} \\ & x_i = x_{min} \; or \; 1 \end{aligned} \tag{1}$$

Where C is the objective function, u is the displacement vector, K is the global stiffness matrix and x_i correspond to the pseudo-density (or design variable) of the ith element varying from x_{min}, which is a user defined parameter, to 1. When x_i assumes value of 1, the ith element is considered a solid element, on the other hand, when x_i assumes value of $x_{min} = 0.001$, the ith element is considered a void element. The target volume is described by V_f, while V_i is the volume of the ith element.

Removing elements from a structure changes the overall structure strain energy ($1/2u^T Ku$). Chu et al. [13] demonstrated that the strain energy from the removed element is directly related to the structure total strain energy change. Additionally, for nonuniform meshes it is necessary to take into account the element volume [14] (V_i) for the calculation of the sensitivity number resulting in elemental strain energy density (α_i) stated as eq. (2).

$$\alpha_i = (\frac{1}{2} u_i^T K_i u_i)/V_i \tag{2}$$

The raw elemental strain energy density is processed to avoid checkerboard patterns in the structure and a mesh-independent solution [15] to achieve these properties the filter scheme is stated as eq. (3).

$$\overline{\alpha_i} = \frac{\sum_{j=1}^{n} W_j \alpha_j}{\sum_{j=1}^{n} W_j} \tag{3}$$

Where W_j is the weight parameter defined as eq. (4).

$$W_j = \begin{cases} r_{min} - r_{ij}, \; when \; (r_{min} - r_{ij}) > 0 \\ 0, \; when \; (r_{min} - r_{ij}) \leqslant 0 \end{cases} \tag{4}$$

Where r_{min} is the user defined filter radius and r_{ij} is the centroid distance from element i to element j. The convergence problem was solved using [16] approach eq. (5):

$$\tilde{\alpha}_i = \frac{(\bar{\alpha}_i^k + \bar{\alpha}_i^{k-1})}{2} \tag{5}$$

Where k is the current iteration. The evolutionary ratio (ER) defines the amount of elements updated per iteration. Usually, ER is a constant value resulting in update always in the same rate. Alternatively, Lin et al. [17] proposes a dynamic evolutionary ratio (eq. (6)), that is, at the beginning of the topological optimization the portion of the removed volume is greater than at the end of the topological optimization

$$ERR_k = \frac{ER_{max} - ER_{min}}{\pi} atan\left(\kappa_1 \frac{V_k - V_f}{V_{full} - V_f} - \kappa_2\right) + \frac{ER_{max} - ER_{min}}{2} \tag{6}$$

Where ERR_k is the dynamic evolutionary ratio, ER_{max} and ER_{min} are the maximum predefined evolutionary ratio and minimum predefined evolutionary, respectively;V_{full} is the initial design domain volume and κ_1,κ_2 are control parameters. V_k is the design domain volume at the kth iteration and it follows the same approach (eq. (7)) used by [16].

$$V_{k+1} = V_k(1 \pm ERR_k) \tag{7}$$

The topology optimization continues until the design domain volume reaches the target volume and eq. (8) is satisfied.

$$error = \frac{\left|\sum_{i=1}^{N} C_{k-i+1} - \sum_{i=1}^{N} C_{k-N+1}\right|}{\sum_{i=1}^{N} C_{k-i+1}} \leqslant \tau \tag{8}$$

Where τ is the convergence error and in this work was set to 0.001. N states the number of iterations of stable compliance set to 5. This work uses Matlab and ANSYS Mecanical to apply the described method and the sequence used in this work follows:

1. MatLab code containing all BESO and FEA parameters starts the simulation, generate an input file containing FEA information and output set up, and starts ANSYS in batch mode;
2. Ansys solves FEA and generates output files containing strain energy and mesh information;
3. MatLab reads the output file, calculates sensitivity number as eq. (2) and filter it as eq. (3);
4. Average sensitivity number as eq. (5) ;
5. Update FEA model with solid and void elements and calculates the next iteration volume using eq. (6)
6. Repeat items; 2,3,4,5 until the design domain volume reach the target volume and eq. (8) is satisfied.

The BESO approach described in this section is applied in a three dimensional 32mm thick Scarifier Subsoiler as defined in Fig. 2.

The forces applied at the tip of the subsoiler, which is 10 mm thicker than the shank, were arbitrary for the sake of simplicity. The material considered was structural steel and, for preliminary analyzes, a 25% reduction in the volume of the subsoiler was considered. The properties of the materials, applied forces, and BESO parameters used are described in the 1.

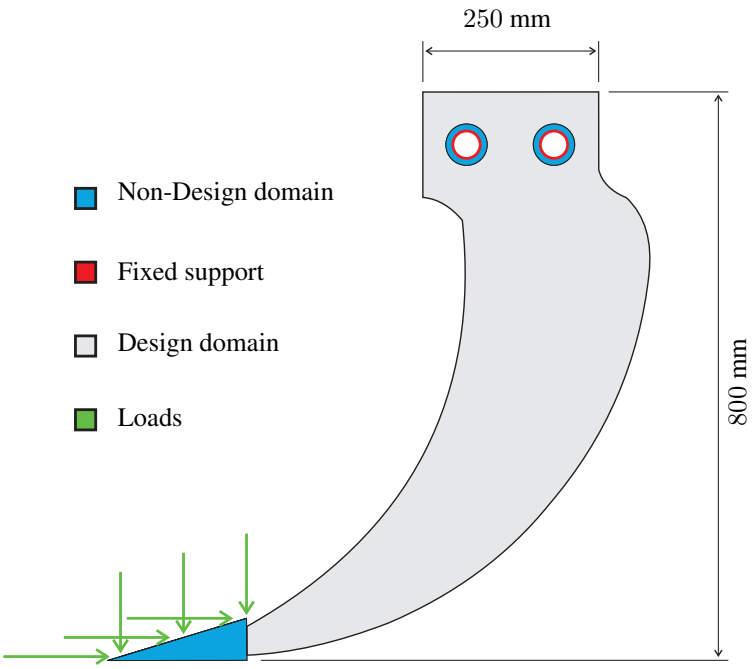

Figure 2. 32 mm thick Scarifier Subsoiler geometry

Table 1. Loads, TO parameters and material properties

Description	Nomenclature	Value
Young's module	E	200 GPa
Poisson's ratio	ν	0.3
Total Vertical force	F_x	5 kN
Total Horizontal force	F_z	10 kN
Final design domain volume	V_f	0.75 V_{full}
Minimum evolutionary rate	ER_{min}	1.0%
Maximum evolutionary rate	ER_{max}	3.0%
Control parameter 1	κ_1	30
Control parameter 2	κ_2	15

3 Results and Discussion

The coupling of the Matlab and ANSYS software brings as main advantages the ability to work with complex geometry problems and speed in finite element analysis. The geometry was created in a 3D CAD software and imported to an ANSYS file. A free 207.949-elements mesh was created in ANSYS and, on average, each finite element analysis took 25.5 seconds in an AMD Rayzen 7 3.6GHz CPU. Such software coupling is especially advantageous since the finite element analysis is performed in a highly known commercial dedicated FEM software, leaving Matlab to manipulate and solve the topology optimization problem.

The main focus of this work is to validate the methodology described in section 2 applied to a subsoiler. During the topology optimization method, the result is dependent on the predefined filter radius. So, a careful analysis of the filter radius is necessary to ensure that the equipment is buildable. Three filters radius were tested, $r_{min} = 10$, 15 and 20. The final topology resulted in each tested filter can be found in Fig. 3 respecting the compliance objective function, and the 25% volume reduction. Most of the removed material was concentrated in the middle and top portion of the subsoiler.

To avoid thin bars and checkerboard problem, the filter radius of $r_{min} = 20$ mm was chosen with a compliance $C = 3722.4$ Nmm, so all the next results and discussions are based on this geometry. The evolution histories

of the objective function is illustrated in Fig. 4. The convergence was satisfied in the last ten iterations in both volume and error, as stated in eq. (8). The material removal occurred in a dynamic evolutionary rate, as stated in eq. (6). Such an approach resulted in fewer iterations and faster convergence.

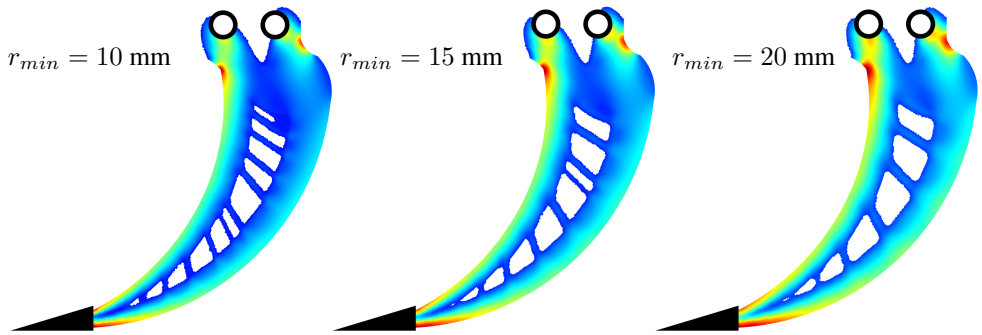

Figure 3. Side view of the final result of topological optimization with radius of $r_{min} = 10, 15$ and 20 mm and filtered sensitivity distribution(cold colors for low elemental sensitivity and hot colors for high elemental sensitivity)

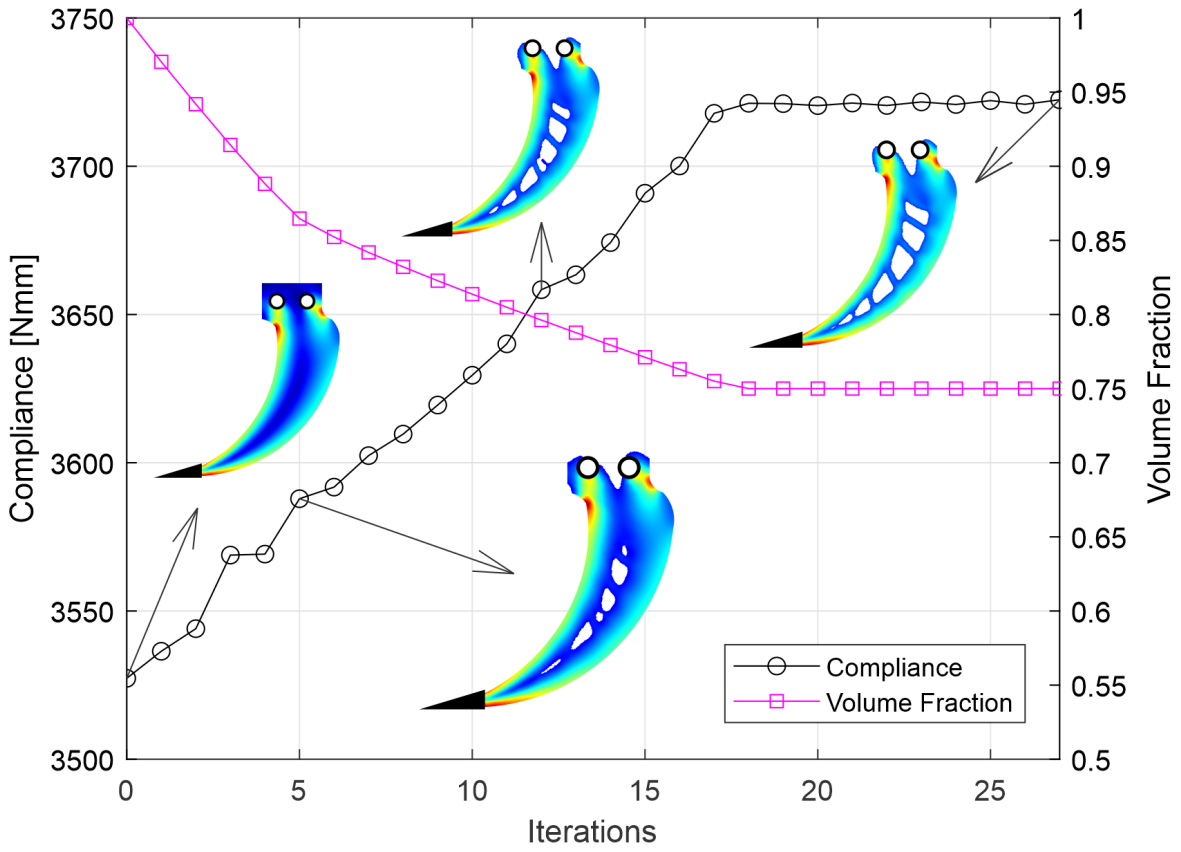

Figure 4. Evolution histories of the volume fraction and compliance

The generation of an adapted geometry based on the final topology optimization geometry is highly depended on the user, since the new geometry is created in a CAD software based in the topology optimization results. This step takes time and in order to guarantee the performance, the volume of the adapted geometry must be equal or greater than the final topology optimization geometry. After the generation of the new geometry, a post-processing

finite element analysis is highly recommended. For the generation of the adapted geometry. The degree of change in geometry depends mainly on the purpose of the change, such as manufacturing, testing, or academic studies. The filtered sensitivity distribution of the adapted geometry is presented in Fig. 4 and the overall reduction and compliance are $V_r = 23.9\%$ and $C = 3721.7$ Nmm, respectively. The compliance from the adapted geometry was slightly lower than resulted from the optimization method.

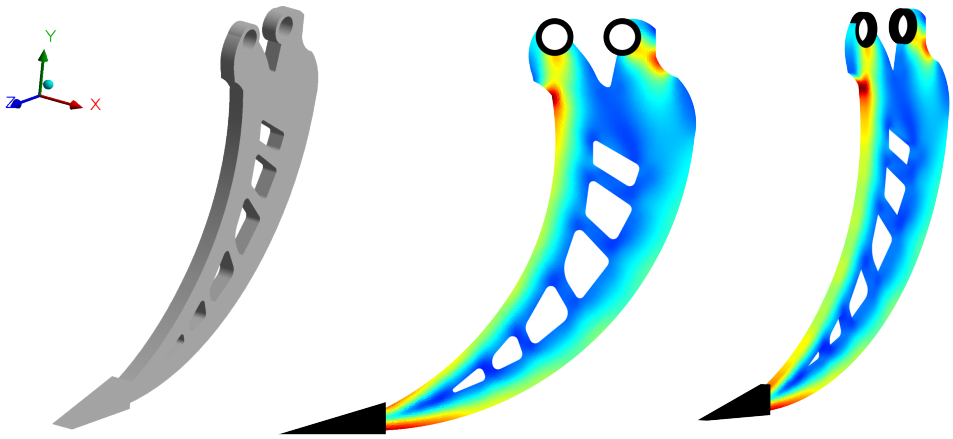

Figure 5. Adapted geometry and filtered sensitivity distribution

4 Conclusion

This initial work presents a methodology to apply the topology optimization procedure in agricultural implements. In future works, the present approach should be extended to consider multi-physics and multi-scale systems in order to modeling the agriculture process more precisely. As a case study, it was considered a topological optimization of a conventional subsoiler shank. The simulation resulted in a reduction of the subsoiler shank with an optimized distribution of material within the initially prescribed work domain. Also, the recent approach of the dynamic evolutionary rate helped to solve the convergence problem and reduced the time spent for each simulation. Since the loads were arbitrary, further studies are needed considering realistic intensity, direction, and sense to guarantee the working performance of the optimized topology. Despite consuming time to generate the adapted geometry it is essential to make the construction of the implement feasible.

Acknowledgements. The present work was financed with support from the National Council for Scientific and Technological Development (CNPq).

Authorship statement. The authors hereby confirm that they are the sole liable persons responsible for the authorship of this work, and that all material that has been herein included as part of the present paper is either the property (and authorship) of the authors, or has the permission of the owners to be included here.

References

[1] Hamzei, J. & Seyyedi, M., 2016. Energy use and input–output costs for sunflower production in sole and intercropping with soybean under different tillage systems. *Soil and Tillage Research*, vol. 157, pp. 73 – 82.
[2] Roger-Estrade, J., Anger, C., Bertrand, M., & Richard, G., 2010. Tillage and soil ecology: Partners for sustainable agriculture. *Soil and Tillage Research*, vol. 111, n. 1, pp. 33 – 40. IZMIR conference (ISTRO 2009).
[3] Cavallo, E., Ferrari, E., Bollani, L., & Coccia, M., 2014. Attitudes and behaviour of adopters of technological innovations in agricultural tractors: A case study in italian agricultural system. *Agricultural Systems*, vol. 130, pp. 44 – 54.
[4] Yurdem, H., Degirmencioglu, A., Cakir, E., & Gulsoylu, E., 2019. Measurement of strains induced on a three-bottom moldboard plough under load and comparisons with finite element simulations. *Measurement*, vol. 136, pp. 594 – 602.

[5] Bendsøe, M. P. & Kikuchi, N., 1988. Generating optimal topologies in structural design using a homogenization method. *Computer Methods in Applied Mechanics and Engineering*, vol. 71, n. 2, pp. 197 – 224.
[6] Xie, Y. & Steven, G., 1993. A simple evolutionary procedure for structural optimization. *Computers & Structures*, vol. 49, n. 5, pp. 885 – 896.
[7] Querin, O., Young, V., Steven, G., & Xie, Y., 2000. Computational efficiency and validation of bi-directional evolutionary structural optimisation. *Computer Methods in Applied Mechanics and Engineering*, vol. 189, n. 2, pp. 559 – 573.
[8] Zhao, Z., Zhou, S., Feng, X., & Xie, Y., 2018. On the internal architecture of emergent plants. *Journal of the Mechanics and Physics of Solids*, vol. 119, pp. 224 – 239.
[9] Dasand, R., Jones, R., & Xie, Y., 2011. Optimal topology design of industrial structures using an evolutionary algorithm. *Optimization and Engineering*, vol. 12, n. 4, pp. 681–717.
[10] Azevedo, F. M., Moura, M. S., Vicente, W. M., Picelli, R., & Pavanello, R., 2018. Topology optimization of reactive acoustic mufflers using a bi-directional evolutionary optimization method. *Structural and Multidisciplinary Optimization*, vol. 58, n. 5, pp. 2239–2252.
[11] Luo, Z., Yang, J., & Chen, L., 2006. A new procedure for aerodynamic missile designs using topological optimization approach of continuum structures. *Aerospace Science and Technology*, vol. 10, n. 5, pp. 364 – 373.
[12] Gao, D., Wang, D., Wang, G., & Hao, L., 2013. Topology optimization of conditioner suspension for mower conditioner considering multiple loads. *Mathematical and Computer Modelling*, vol. 58, n. 3, pp. 489 – 496. Computer and Computing Technologies in Agriculture 2011 and Computer and Computing Technologies in Agriculture 2012.
[13] Chu, D., Xie, Y., Hira, A., & Steven, G., 1996. Evolutionary structural optimization for problems with stiffness constraints. *Finite Elements in Analysis and Design*, vol. 21, n. 4, pp. 239 – 251.
[14] Huang, X. & Xie, Y., 2010. *Bi-Directional Evolutionary Structural Optimization Method*, chapter 3, pp. 17–38. John Wiley & Sons, Ltd.
[15] Sigmund, O., 2007. Morphology-based black and white filters for topology optimization. *Structural and Multidisciplinary Optimization*, vol. 33, n. 4, pp. 401–424.
[16] Huang, X. & Xie, Y., 2007. Convergent and mesh-independent solutions for the bi-directional evolutionary structural optimization method. *Finite Elements in Analysis and Design*, vol. 43, n. 14, pp. 1039 – 1049.
[17] Lin, H., Xu, A., Misra, A., & Zhao, R., 2020. An ansys apdl code for topology optimization of structures with multi-constraints using the beso method with dynamic evolution rate (der-beso). *Structural and Multidisciplinary Optimization*.